

Thermal Properties and Miscibility of Semi-Crystalline and Amorphous PLA Blends

Chengcheng Gao,^{1,2,3} Xianyang Bao,¹ Long Yu,¹ Hongsheng Liu,¹ George P. Simon,³ Ling Chen,¹ Xingxun Liu¹

¹Centre for Polymer from Renewable Resource, ERCPS, South China University of Technology, Guangzhou 510641, People's Republic of China

²CSIRO, Materials Science and Engineering, Melbourne, Vic. 3169, Australia

³Department of Materials Engineering, Monash University, Clayton, Vic. 3800, Australia

Correspondence to: L. Yu (E-mail: felyu@scut.edu.cn) and H Liu (E-mail: liuhongsheng@scut.edu.cn)

ABSTRACT: The focus of this research is the study of the microstructures and miscibility at the interface between semi-crystalline and amorphous PLAs [poly (L-lactic acid)(PLLA) with poly (L,D-lactic acid)(PDLLA), respectively]. The blends are prepared through thermal processing (extrusion and hot-pressing). To increase the area of interface between PDLLA and PLLA, the fibers from PLLA and PDLLA are used. Thermal and microstructures of the blends were studied by differential scanning calorimetry (DSC), polarized optical microscopy (POM), dynamic thermogravimetric analysis(DMA), small-angle X-ray diffraction(SAXS) and wide-angle X-ray diffraction (WAXD). The two PLAs are miscible in molten state. However, phase separation is detected after various thermal treatments, with PDLLA being excluded from the regions of interlamellar PLLA regions when PDLLA content is low, as determined from X-ray diffraction studies. The compatibility between the two PLAs is not perfect in the molten state, since enthalpies of the various blends at T_g are lower than any pure PLA material. The semi-crystalline PLLA fiber can recrystallize alone in the molten amorphous PDLLA, and a higher nuclei density is observed at the interface. © 2014 Wiley Periodicals, Inc. *J. Appl. Polym. Sci.* **2014**, *131*, 41205.

KEYWORDS: biopolymers and renewable polymers; blends; structure-property relations

Received 8 April 2014; accepted 22 June 2014

DOI: 10.1002/app.41205

INTRODUCTION

Miscibility of components in polymer blends has attracted great attention because it is usually a key factor in determining the performance of blends.^{1,2} Because miscibility is a thermodynamic concept, it is meaningful only under equilibrium conditions, and thus the study of miscibility in the liquid state is thermodynamically more valid than that its study in the solid state where kinetics also plays a role. A special group of polymer blends which have various levels of miscibility are those when the constituent polymers are from same chemical component, such as the blends of isotactic polypropylene (iPP) with amorphous polypropylene (aPP), the blends of high density polyethylene (HDPE) with low density polyethylene (LDPE),³ the blends of isotactic polystyrenes (iPS) with syndiotactic polystyrenes (sPS)⁴ and the blends of PLLA with poly (D-lactic acid) (PDLA). The miscibility of this kind of polymer blends has attracted much attention, since the similarity of chemical components could increase polymeric knowledge to understand the miscibility of polymer blends more broadly. The study of miscibility of this kind of polymer blends is not only of scientific interest, but also has industrial importance, an example being

the development of self-reinforced composites (SRCs), or single-polymer composites in which a polymer matrix is reinforced by the reinforcing agents, such as particles or fibers from same polymer.⁵⁻⁹ This is particularly of interest where both components are biodegradable (such as in this work), because the final composite may show the kinds of benefits of incorporation of composite fibers, whilst the blend also remains biodegradable.

For this kind of polymer blend, the most extensively investigated system involves blends of HDPE/LDPE, which have previously been reviewed.¹⁰ Generally, they are considered as miscible in the molten state, with phase separation observed during solidification. It is believed that the subsequent immiscibility is attributed to the differences in the interaction energies of CH₂, CH₃, and CH groups, which result in different crystallization rates. Another popular polyolefinic blend that of iPP combined with amorphous components aPP has also received much attention because aPP is a noncrystallizable component that cannot exist in the crystalline lattice of iPP. The location of the amorphous aPP chains can be divided into three size scales: interspherulitic (where the aPP phase is located at the

spherulitic boundaries, and is completely excluded from the growing spherulites), interfibrillar, and interlamellar segregation.

Compared with polyolefins, there is much less reports relating to polyester blends in which the polymers contain the same chemical component. PLA is one of the few kinds of polyester that has been studied in such a way. The blends of enantiomeric PLAs, PLLA and PDLA, can result in a higher melt temperature because a stereocomplex is formed due to the strong interactions between PLLA and PDLA chains.^{11–13} Moreover, PLLA/PDLA blends have a higher hydrolysis resistance compared with that of pure PLLA and PDLA, even when it is amorphous, again due to the strong interaction between PLLA and PDLA chains.^{14,15} On the other hand, PLLA comprises isotactic sequences which are crystallizable, whereas PDLA is composed of a racemic mixture of L- and D-lactides and is thus amorphous.¹⁶ PLLA is usually hard and brittle which hinders its usage in many applications. Blending PLLA with amorphous PDLA can improve the toughness of PLLA.¹⁷ Furthermore; PDLA can degrade quickly due to its amorphous structure. Thus, the degradation time of PLLA/PDLA blends can be controlled through various blending ratios. The miscibility of PLLA/PDLA blends has been extensively studied.^{18–21} As for most polyesters, the thermal behaviors of PLA are much more complex than that of polyolefins. A number of key thermal events such as glass transition T_g , cold crystallization T_{cc} and melting T_m , as well as crystallization T_c during cooling have all been reported.²²

Tsuji et al.¹⁹ have discussed the effects of mixing ratio on crystallization. The crystallization of PLLA takes place in the PLLA/PDLA blends from the melt when the PLLA content is high. The morphology of spherulites becomes increasingly disordered with a decrease in PLLA content, explained by the fact PDLA chains must be trapped between the lamellae in spherulites but not in the boundaries of the spherulites when the PLLA content is higher. Bouapao et al.²³ have found that the quenched blends exhibit two glass transitions, which demonstrate that PLLA and PDLA are immiscible and phase-separated in their blend films. Long periods associated with the lamellae stacks measured by SAXS and T_m shows that PDLA chains are excluded from the PLLA lamellae and the interlamellar amorphous region during the crystallization process. The excluded PDLA chains should have yielded amorphous domains as dark spots in spherulite. The large amount of PDLA surrounding PLLA could disturb the formation of PLLA crystallite nuclei or the growth of PLLA crystallites in the limited crystallization period. Chen et al.²⁴ also reported that the PLLA/PDLA blends have two T_g measured by both DSC and DMA.

The ultimate aim of this work is to develop PLA-based self-reinforced composites in which using PLA fiber to reinforce PLA matrix. To this end, we have studied here the microstructures and miscibility focusing on the interface between semicrystalline PLLA fiber and amorphous PDLA matrix. Morphologies, thermal properties, and interface between semi-crystalline and amorphous PLA blends were all investigated through both melt blending and hot compression implementing at a temperature that is higher than the glass transition temperature but less

than the melt temperature of the two components. To increase the interface area between each component, the fibers from semicrystalline and amorphous PLAs were used.

EXPERIMENTAL

Materials and Specimen Preparation

Commercially available PLLA and PDLA were supplied in pellet form by NatureWorks, their trade names are PLA 4302 and PLA 6302, respectively. They were dried at 65°C for 24 h in a vacuum oven before processing.

Melt spinning of the fiber was carried out on a Busschaert bicomponent system that contains a single screw extruder connected by a spin block.²⁵ The multifilament bundle was produced by melt extrusion and passed through a vertical air-quenching system. The cooling of the filaments was optimized by passing the multi filament bundle through a distance of 5–6 m at a take-up speed of 500 m min⁻¹ whilst being coated with finish oil to decrease friction on the godets station during the cold drawing process. Both PLLA and PDLA fibers were produced under the same conditions.

The specimens from melt blending were prepared by first compounded using a Haake co-rotating twin-screw extruder (Rheomex PTW 24/40p, $\Phi = 30$) in different PLLA/PDLA ratios (w/w): 100/0, 80/20, 60/40, 40/60, 20/80, 0/100 with highest barrel temperature 190°C, from zone 1 to 9: 60, 120, 170, 190, 190, 190, 180, and 180°C (die). The compounded pellets were extruded using a Haake single-screw extruder ($\Phi = 30$) with a sheet die (60 mm width) at highest barrel temperature 180°C to prepare film with 0.1 mm thickness. The PDLA films used for polarized light microscopy analysis were extruded using same extruder under same conditions. The specimens from hot compression were prepared by mixing short PLLA and PDLA fibers (50/50, w/w) manually at room temperature, and then pressed at 80°C under 2 tons for 5 min in a plate hot-presser.

Microstructure Characterization

A microscope with polarization capabilities (Nikon Eclipse 80i) equipped with a hot stage (Linkam CSS 450) was used to study the crystallization behavior of the blends. Samples were heated from room temperature to 200°C at a speed of 30°C min⁻¹ and held for 5 min, then cooled to 120°C at a speed of 30°C min⁻¹ to allow isothermal crystallization. The interval for taking optical micrographs was set at 20 s to capture images during the isothermal crystallization process. In this work the magnification 50 × 10 was used. The measurement of diameter variations of spherulite was conducted using a NIS-Elements BR 2.20 system.

A SAXSess (Anton-Paar, Graz, Austria) was used as both wide angle X-ray scatter (WAXS) and small angle X-ray scatter (SAXS) facility. A PW3830 X-ray generator with a long fine focus sealed glass X-ray tube (PANalytical) was operated at 40 kV and 50 mA. A focusing multilayer optics and a block collimator provide an intense monochromatic primary beam (Cu K α , $\lambda = 0.1542$ nm). The 2D data were integrated into the one-dimensional scattering function $I(q)$ as a function of the magnitude of the scattering vector q defined as: $q = 4\pi\sin\theta/\lambda$, where λ is the wavelength and 2θ is the scattering angle.

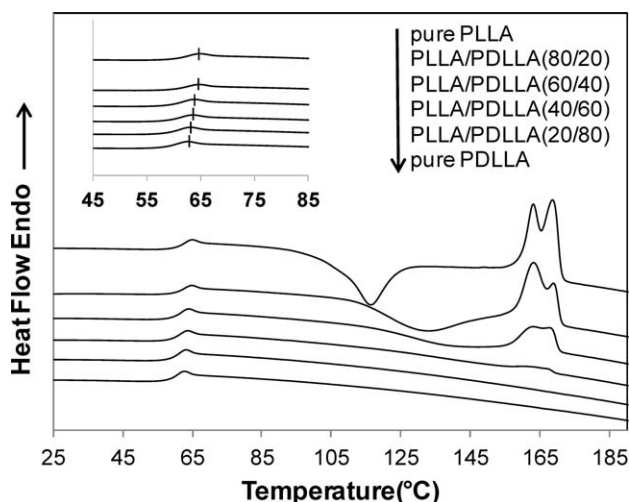


Figure 1. DSC heating curves ($20^{\circ}\text{C min}^{-1}$) of quenched PLLA/PDLLA blends. The inset shows their magnified glass transition temperature.

Thermal Properties

A Perkin-Elmer DSC 8500 with a liquid cooling system and nitrogen purge gas was used in the experimental work to study the thermal properties of PLLA and PDLLA blends. The samples (~ 5 mg) were weighed and sealed in an aluminum pan. To study cold-crystallization, the samples were cooled to 0°C with a cooling rate of $100^{\circ}\text{C min}^{-1}$ after melting at 200°C for 3 min. They were then heated to 200°C at a speed of $20^{\circ}\text{C min}^{-1}$. In the case of melt-crystallization, after melting at 200°C for 3 min, the samples were then cooled to 25°C at $2^{\circ}\text{C min}^{-1}$. Triple measurements were carried for each samples, and the average result was reported, along with the standard deviation.

A Perkin-Elmer Pyris Diamond DMA was used to study the dynamic mechanical properties of the blends. Specimens of dimension 8 mm (wide) \times 20 mm (long) \times 0.15 mm (thick) were used in the experimental. The system was run in the rectangular tension mode at 1 Hz, with a temperature range of between 25 and 170°C at a heating rate of $2^{\circ}\text{C min}^{-1}$.

RESULTS AND DISCUSSION

Miscibility of PLLA/PDLLA Blends Prepared by Melting Blending

Figure 1 shows the DSC heating curves of quenched PLLA/PDLLA blends with different ratios. The blends show typical

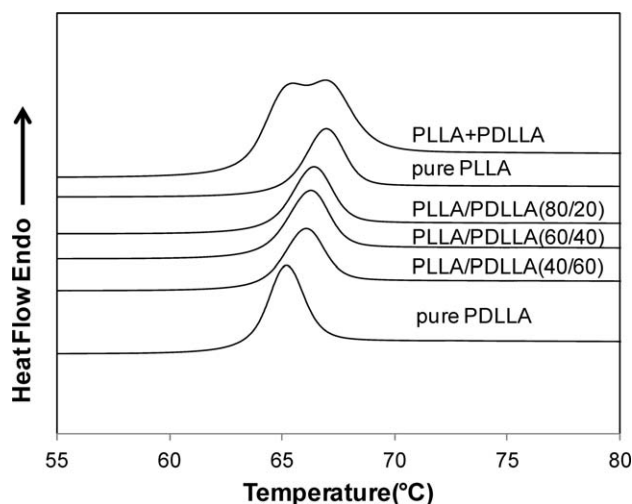


Figure 2. DSC thermograms of quenched PLLA/PDLLA blends after thermal treatment at 45°C for 17 h.

semicrystalline thermal behaviors of PLLA: glass transition, cold crystallization and two melting peaks for α and β -types crystals,²² while only one glass transition temperature was detected relating to amorphous PDLLA. Table I lists these key temperatures determined by DSC. All the blends with different compositions exhibited a single T_g that shifted to a lower temperature with an increase in the PDLLA content, which could indicate that PLLA and PDLLA are miscible in molten state. The cold crystallization temperature, T_o increased as the PDLLA content increased. That may because of PDLLA chains presenting in PLLA-rich phase retarding the crystallization of PLLA, which also indicates that the two PLAs are miscible in molten state. The enthalpies of both cold crystallization and melting of PLLA decreased with increasing amount of PDLLA, likely due to the fact that PDLLA decreased the number of nuclei and diluted PLLA in molten state.²⁶ This means extra energy is required for PLLA chains separating from PDLLA chains and transporting to the growth front of PLLA crystal lamella.²¹ The double melting peaks in such systems are not indicative of multiple crystallizable phases but have been explained by a melting, recrystallization, and remelting mechanism of the PLLA.^{27,28} The Peak-1 at lower temperature is the melting peak of crystal existing in the solid PLLA, while the Peak-2 represents the melting peak of crystal forming during heating (in particular at the melting

Table I. Thermal Parameters of Various PLLA/PDLLA Blends Prepared by Quenched from Melting

PLLA/PDLLA	T_g ($^{\circ}\text{C}$)	ΔH_c (J g^{-1})	T_{cc}^a ($^{\circ}\text{C}$)	ΔH_c^c (J g^{-1})	T_{m1}^b ($^{\circ}\text{C}$)	T_{m2}^b ($^{\circ}\text{C}$)	ΔH_m^c (J g^{-1})
100/0	61.1 ± 0.7	1.35 ± 0.31	107.0 ± 0.8	31.83 ± 3.71	163.0 ± 0.4	168.6 ± 0.8	36.12 ± 1.62
80/20	60.8 ± 0.6	1.37 ± 0.27	116.3 ± 1.5	23.93 ± 1.13	163.1 ± 0.7	167.8 ± 0.3	25.53 ± 1.13
60/40	59.8 ± 0.3	1.30 ± 0.14	126.1 ± 1.7	09.02 ± 0.82	163.1 ± 0.3	167.7 ± 0.2	12.61 ± 0.62
40/60	59.7 ± 0.5	1.33 ± 0.21	-	-	162.5 ± 0.6	167.0 ± 0.6	1.84 ± 0.71
20/80	59.2 ± 0.7	1.39 ± 0.13	-	-	-	-	-
0/100	58.8 ± 0.5	1.38 ± 0.24	-	-	-	-	-

^a T_{cc} is onset temperature of cold crystallization.

^b T_{m1} and T_{m2} is the melt temperature of the peak at low temperature and high temperature, respectively.

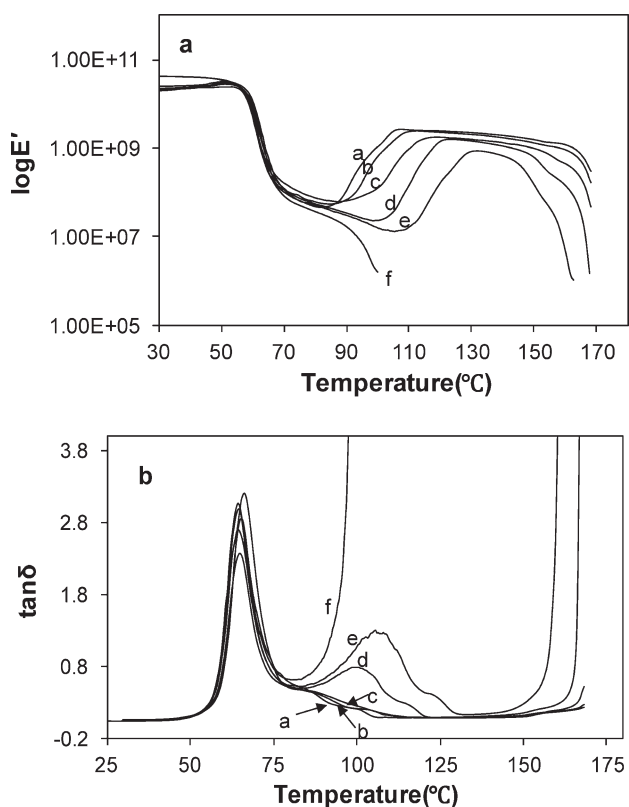
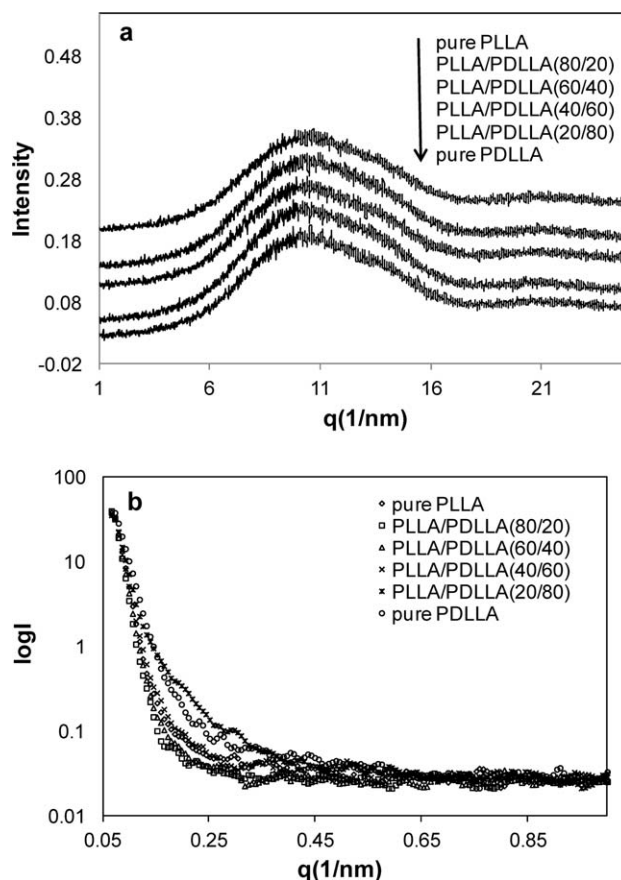
^c Both ΔH_c and ΔH_m were calculated based on pure PLLA.

Table II. Thermal Parameters of PLLA/PDLLA Blends at T_g in Which Samples were Annealed at 45°C for 17 h

PLLA/PDLLA ratio	T_g (°C)	ΔC_p ($J g^{-1} °C$)	ΔH_r ($J g^{-1}$)
100/0	64.2 ± 0.21	0.58 ± 0.07	5.3 ± 0.27
80/20	63.9 ± 0.17	0.46 ± 0.02	5.2 ± 0.32
60/40	63.6 ± 0.24	0.40 ± 0.08	4.7 ± 0.42
40/60	63.5 ± 0.34	0.37 ± 0.12	4.4 ± 0.37
0/100	62.9 ± 0.18	0.48 ± 0.08	5.4 ± 0.42

point of the PLLA). Compared with the pure PLLA, the area ratio of Peak-1/Peak-2 increased, which indicates that crystals with higher stability (β crystal) formed during the recrystallization (during heating) was decreased in the presence of PDLLA acting as diluents.²¹

An endothermic peak at T_g (representing excess enthalpy relaxation) was detected for both the semi-crystalline and amorphous PLAs. The enthalpy represents the degree of packing of the amorphous chains and has been widely used to study ageing, density and distance of polymers from equilibrium.^{2,18,26} By looking at aspects of enthalpy of relaxations of polymer mixtures, it is expected that aspects of miscibility can be determined, particularly if their glass transition temperature is close. To enlarge the relaxation peak at glass transition, samples were

**Figure 3.** Storage modulus (E'_c) and $\tan \delta$ of various PLLA/PDLLA blends: (a) pure PLLA, (b) 80/20, (c) 60/40, (d) 40/60, (e) 20/80, and (f) pure PDLLA measured by DMA scanned at $2^\circ C min^{-1}$.**Figure 4.** WAXS and SAXS of PLLA/PDLLA blend with different ratios.

annealed at 45°C for 17 h. Figure 2 shows the DSC thermograms of different PLLA/PDLLA blends after the thermal treatment. A mixed sample after hot-pressed at the temperature lower than their melting temperatures, PLLA + PDLLA (50/50 w/w), was also studied as a comparison. Samples quenched from the molten to the solid state have been used to study the phase behaviors representing melting state.²⁹ For all the melt-blending samples, DSC scans shows only one enthalpy peak, and the relatively sharp endothermic peak indicates that PLLA and PDLLA may be miscible. It was found that the PLLA shows higher temperatures for both T_g and the relaxation peak, compared with the PDLLA. Both the T_g of the aged materials and the peak temperature increased with increasing PLLA content. The PLLA+PDLLA blend shows two corresponding enthalpy relaxation peaks in Figure 2. Table II gives the detailed results of the thermal parameters of different blends at T_g . It was found that both the glass transition temperature and relaxation peak were slightly increased after annealing (compared with quenched data), which is expected, since the annealing treatment increased density as the chains became more tightly packing and thus there is greater enthalpy relaxation on rescanning. It is interesting to notice that the enthalpies (ΔH) of the various blends are lower than any pure PLA material. That means that the compatibility between the two PLAs is not perfect, or at least the crystals from the blends are not as good as individual polymer itself, even if they are miscible in melting state.

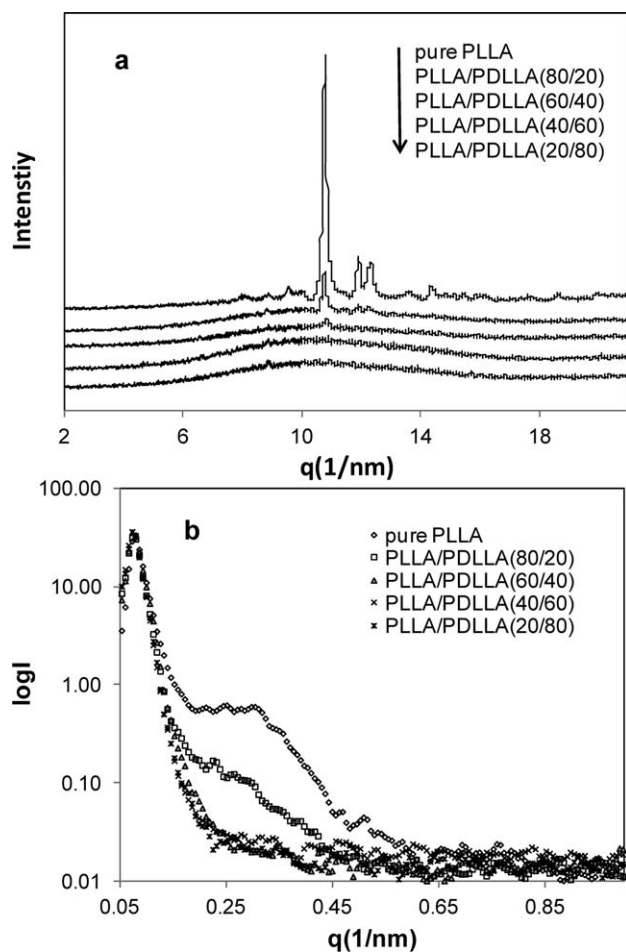


Figure 5. WAXS and SAXS of PLLA/PDLLA blends after thermal treatment at 120°C for 20 min.

Figure 3 exhibits the temperature dependence of storage modulus (E') and $\tan \delta$ curves of various PLLA/PDLLA blends determined by DMA. It is seen that PLLA and PDLLA, as well as various blends show a similar pattern. The E' values of all the specimens decreased sharply at around 60°C, and there is a $\tan \delta$ peak near 64°C, which is clearly the dynamic glass transition temperature of PLAs. The peak temperature of $\tan \delta$ is slightly decreased with increasing PDLLA content, as with the results of the DSC (see Table I).

Above the glass transition temperature, a significant increase of storage modulus was observed during the continued heating at above T_g for all the specimens, except pure PDLLA. The onset temperatures corresponding to the increase in E' values shift to higher temperatures with increasing PDLLA content in blends. The increase in E' values of PLA specimens at above T_g was attributed to the cold crystallization of the PLLA in the blends during the increasing temperature scanning. Because PLLA needs more energy to form an ordered structure when PDLLA is present, the onset temperature thus increased,³⁰ as was observed for the exotherm onsets in Figure 1 DSC data. Obviously, the cold crystallization is much more readily observed in the DMA data than that of DSC. It should also be noted that the temperature region of crystallization at above T_g becomes narrower with increasing PDLLA content.

Following the glass transition, the value of $\tan \delta$ increased with increasing temperature, although the increased trend varied depending on the ratio of the two kinds of PLAs. For the pure PDLLA, the $\tan \delta$ increased rapidly since the specimen became molten and thus viscous. In the PDLLA-rich blends, the $\tan \delta$ increased first and subsequently decreased with increasing temperature, the breadth of the peak also increased with increasing PDLLA content. This was due to the fact that small amounts of ordered structure formed during the heating, which hindered $\tan \delta$ continuously increasing. In the PLLA-rich blends, the $\tan \delta$ remained constant until the specimens melted. This was due to ordered structure limiting the mobility of the polymer chains in amorphous phase and thus reducing its mechanically lossy motions.

Figure 4 shows WAXS and SAXS of quenched PLLA/PDLLA blends with different ratios. It can be observed that all samples show a similar pattern. There was no difference observed for all samples at different scattering angles, and no crystals and long-range ordered structure were detected for all PLLA and PDLLA blends, indicating that all of the specimens are amorphous. As shown in Figure 4(b), the scattering intensity in small q regions was very weak and showed no apparent difference for all samples, which indicates the distribution of electron density in various PLLA/PDLLA blend was homogeneous. Figure 5 shows X-ray diffraction patterns of various PLLA/PDLLA blends after isothermal annealing at 120°C for 20 min. It is seen that a strong peak and several weak peaks are observed for pure PLLA.

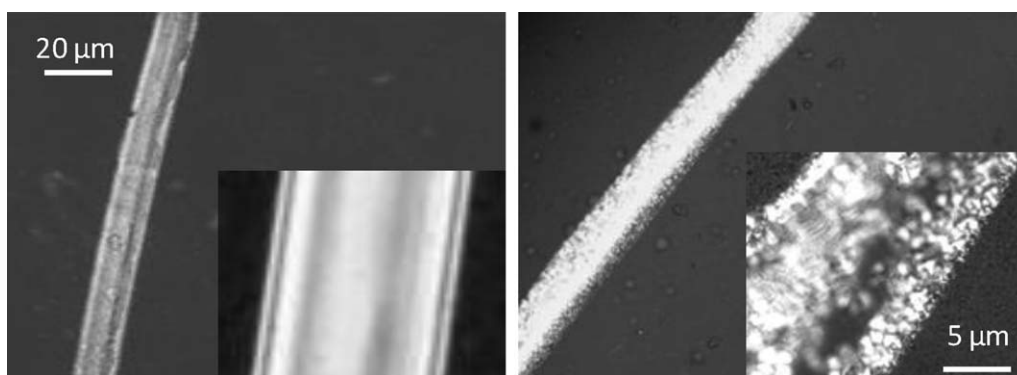


Figure 6. Semi-crystalline PLLA in the amorphous PDLLA matrix after heating to 140°C (left) and 120°C (right) cooling from 200°C.

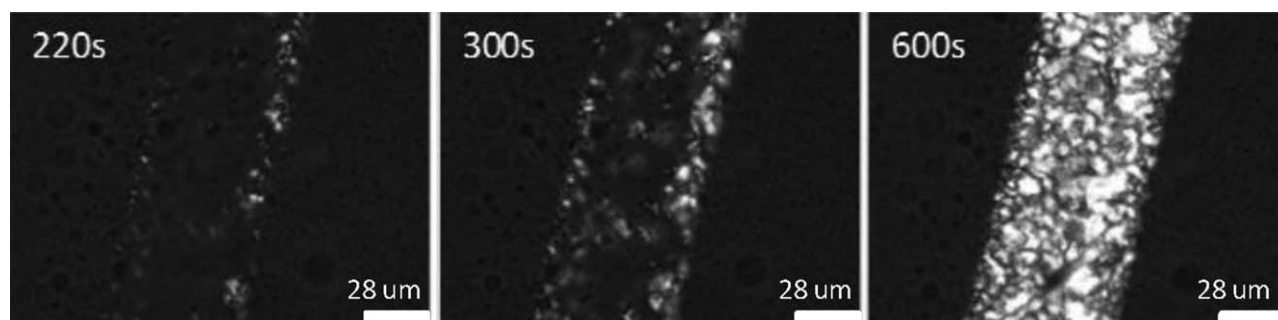


Figure 7. POM micrographs of the interface between the PLLA fiber and PDLLA matrix during isothermal crystallization at 120°C.

The crystalline peaks were less obvious in blends incorporating PDLLA. It has been found that the maximum scattering vector (q_{\max}) appeared at about 0.3 for PLLA and only for the blend of PLLA 80/PDLLA 20. The q_{\max} is usually used to calculate long period, $L(q_{\max}) = 2\pi/q_{\max}$. For PLLA, the L value obtained in the present study was about 209 Å, similar to the value of 200–250 Å reported by Baratian et al.³¹ The L value of PLLA 80/PDLLA 20 blend is almost the same as that of pure PLLA, which means that PDLLA chains are not included within the PLLA interlamellar region, even for the blends containing low PDLLA content. When the PDLLA content is high, the difference of electron density cannot generate a SAXS signal and the L does not occur. The results indicate that phase separation occurred during the thermal treatment, which corresponds to the DSC results.

Crystallization Properties of PLLA at the Interface Between PLLA and PDLLA

It is well known that in the most immiscible blends, the second phase affects the overall crystallization rate through its influence on nucleation rate, while the spherule growth rate is usually independent of the presence of the second component.²³ To understand the effect of PDLLA on the crystallization of PLLA in immiscible state, the effect of interface between PLLA and PDLLA on the nucleation of PLLA was investigated by DSC and polarize microscope.²³ To investigate the immiscible system and enlarge the interface between PDLLA and PLLA, PLLA fibers (50/50 w/w) were used. The preparation method was described in the preparation section. Figure 6 shows the semi-crystalline PLLA fiber in the amorphous PDLLA matrix after heating to 140 and 120°C cooling from 200°C, respectively. It can be seen that the thermal treatment at 140°C did not change the morphology and microstructure of the PLLA fiber. Birefringence, diagonal line and thickness value of the diagonal line for the fiber remained almost the same, which provides an operational window for preparing PLA-based self-reinforced composites. When the treatment is above the melting temperature, the PLLA fiber can recrystallize separately in the molten PDLLA and retain its fiber morphology. Figure 7 shows the isothermal cold crystallization of PLLA in the PDLLA at 120°C. The PLLA fiber and PDLLA film were heated to 200°C first, then cooled to 120°C to let PLLA crystallize in the PDLLA. It can be seen that the PLLA crystallized firstly at the interface between PLLA

and PDLLA. This result indicates that the presence of the PDLLA promoted the formation of heterogeneous nuclei.

To confirm the arguable heterogeneous nucleation for PLA systems since different phenomenon were observed in polypropylene systems,^{32,33} we have carried out some DSC works. Figure 8 shows DSC heating and cooling curves of pure PLLA and PLLA+PDLLA (50/50) blends, respectively. It can be seen from

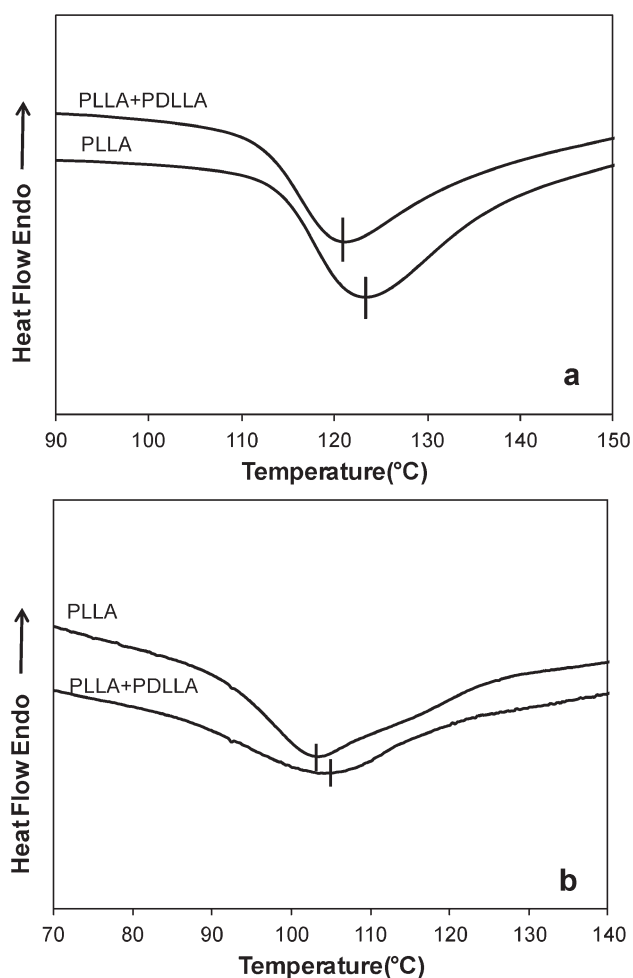


Figure 8. DSC curves of the pure PLLA and PLLA/PDLLA (50/50) fiber blend: (a) heating from the glass state (at 20°C min⁻¹); (b) cooling from the molten state (at 2°C min⁻¹).

Figure 8(a) that the cold crystallization peak temperature of PLLA decreased about 3°C after blending with PDLA, while Figure 8(b) shows that the melting crystallization peak temperature of PLLA increased about 1°C after contacting with PDLA when the sample cooling from molten state. That indicates the interface between PLLA and PDLA can provide nuclei centre.

CONCLUSIONS

Semicrystalline PLLA and amorphous PDLA blends were prepared through both melt blending and hot-pressing, and PLA fibers were used to increase the area of interface. It was found that the two PLAs are miscible in the molten state, which is preserved when quenched. However, the compatibility between the two PLAs is not perfect in the molten state. Phase separation could be detected after various thermal treatments in the solid state. For example, the crystal peaks of PLLA were detected by WAXS; and PDLA chains were excluded from the PLLA interlamellar region as measured by SAXS after blended samples annealing at cold crystallization temperature (120°C).

The presence of PDLA reduced PLLA crystallinity and retarded reorganization of the more stable crystal (the second melting peak). The PLLA fiber can recrystallize alone in the molten amorphous PDLA, and a higher density of nuclei was observed on the interface. DSC results also support that the interface between PLLA and PDLA can provide nuclei centre.

ACKNOWLEDGMENTS

The authors from SCUT, China, acknowledge the research funds NFSC (21174043, 31301554) and GDCXY (2012B091000098). C. Gao acknowledge the State Scholarship Fund provided by the China Scholarship Council supporting her studies in Australia.

REFERENCES

1. Robeson, L. M. *Polym. Eng. Sci.* **1984**, *24*, 587.
2. Hong, B. K.; Jo, W. H.; Kim, J. *Polymer* **1998**, *39*, 3753.
3. Hamee, T.; Hussein, I. A. *Macromol. Mater. Eng.* **2004**, *289*, 198.
4. Li, S. H.; Woo, E. M. *Macromol. Mater. Eng.* **2006**, *291*, 1397.
5. Gao, C.; Yu, L.; Liu, H.; Chen, L. *Prog. Polym. Sci.* **2012**, *37*, 767.
6. Karger-Kocsis, J.; Bárány, T. *Compos. Sci. Technol.* **2014**, *92*, 77.
7. Kmetty, Á.; Bárány, T.; Karger-Kocsis, J. *Progr. Polym. Sci.* **2010**, *35*, 1288.
8. Jia, W.; Gong, R. H.; Hogg, P. J. *Comp. B* **2014**, *62*, 104.
9. Gurarlan, A.; Tonelli, A. E. *Polym. Prep.* **2011**, *52*, 186.
10. Zhao, L. Y.; Choi, P. *Mater. Manuf. Process.* **2006**, *21*, 135.
11. Ikada, Y.; Jamshidi, K.; Tsuji, H.; Hyon, S. H. *Macromolecules* **1987**, *20*, 904.
12. Tsuji, H.; Fukui, I. *Polymer* **2003**, *44*, 2891.
13. Tsuji, H.; Ikada, Y. *Polymer* **1999**, *40*, 6699.
14. Tsuji, H. *Polymer* **2002**, *43*, 1789.
15. Tsuji, H.; Ikada, Y. *Macromolecules* **1992**, *25*, 5719.
16. Liao, X.; Nawaby, A. V. *Ind. Eng. Chem. Res.* **2012**, *51*, 6722.
17. Chen, C. C.; Chueh, J. Y.; Tseng, H.; Huang, H. M.; Lee, S. Y. *Biomaterials* **2003**, *24*, 1167.
18. Ren, J. D.; Adachi, K. *Macromolecules* **2003**, *36*, 5180.
19. Tsuji, H.; Ikada, Y. *J. Appl. Polym. Sci.* **1995**, *58*, 1793.
20. Tsuji, H.; Ikada, Y. *Polymer* **1996**, *37*, 595.
21. Pan, P.; Liang, Z.; Zhu, B.; Dong, T.; Inoue, Y. *Macromolecules* **2009**, *42*, 3374.
22. Yu, L.; Liu, H.; Dean, K. *Polym. Int.* **2009**, *58*, 368.
23. Bouapao, L.; Tsuji, H.; Tashiro, K.; Zhang, J.; Hanesaka, M. *Polymer* **2009**, *50*, 4007.
24. Chen, J. H.; Chang, Y. L. *J. Appl. Polym. Sci.* **2006**, *103*, 1093.
25. Gao, C.; Ma, H.; Liu, X.; Yu, L.; Chen, L.; Liu, H.; Li, X.; Simon, G. P. *Polym. Eng. Sci.* **2013**, *53*, 976.
26. Yu, L.; Liu, H.; Dean, K.; Chen, L. *J. Polym. Sci. B Polym. Phys.* **2008**, *46*, 2630.
27. Zhang, Y.; Deng, B.; Liu, Q.; Chang, G. *J. Macromol. Sci., B Phys.* **2012**, *52*, 334.
28. Sweet, G. E.; Bell, J. P. *J. Polym. Sci. B Polym. Phys.* **1972**, *10*, 1273.
29. Bartczak, Z.; Galeski, A.; Martuscelli, E. *Polym. Eng. Sci.* **1984**, *24*, 1155.
30. Yeh, J. T.; Tsou, C. H.; Huang, C. Y.; Chen, K. N.; Wu, C. S.; Chai, W. L. *J. Appl. Polym. Sci.* **2010**, *116*, 680.
31. Baratian, S.; Hall, E. S.; Lin, J. S.; Xu, R.; Runt, J. *Macromolecules* **2001**, *34*, 4857.
32. Varga, J.; Karger-Kocsis, J. *J. Mater. Sci. Lett.* **1994**, *13*, 1069.
33. Varga, J.; Karger-Kocsis, J. *Polym. Sci. Phys.* **1996**, *34*, 657.